

A tetragonal form of dysprosium orthomolybdate at room temperature

Sesegma Dorzhieva,^a Ihor Chumak,^b Angelina Sarapulova,^{b*} Daria Mikhailova,^b Jibzema Bazarova^a and Helmut Ehrenberg^c

^aBaikal Institute of Nature Management, Siberian Branch of the Russian Academy of Sciences, Sakhyanova Street 6, Ulan-Ude, Russian Federation, ^bInstitute for Complex Materials, IFW Dresden, Helmholtzstrasse 20, 01069 Dresden, Germany, and ^cKarlsruhe Institute of Technology (KIT), Institute for Applied Materials (IAM), Hermann-von-Helmholtz-Platz 1, D-76344 Eggenstein-Leopoldshafen, Germany
Correspondence e-mail: a.e.sarapulova@ifw-dresden.de

Received 15 June 2011

Accepted 18 August 2011

Online 15 September 2011

In the present tetragonal modification of dysprosium orthomolybdate, $\text{Dy}_2(\text{MoO}_4)_3$, the Dy, one Mo and one O atom are located on a mirror plane with Wyckoff symbol 4e, while another Mo atom is located on a fourfold inverse axis, Wyckoff symbol 2a. A single crystal was selected from a polycrystalline mixture of the $\text{Dy}_2\text{O}_3\text{--ZrO}_2\text{--MoO}_3$ system and was stable at room temperature for at least three months. The structure refinement does not indicate the presence of Zr on the Dy sites (to within 1% accuracy). Thus, the stabilization of the tetragonal form is due to disordered positions for a second O atom and split positions for a third O atom that also maintain the DyO_7 coordination, which is not expected for short Dy–O distances [2.243 (6)–2.393 (5) Å].

Comment

It is known that the molybdates of the rare earth elements show interesting fluorescence, laser, piezoelectric, ferroelectric and ferroelastic properties, and they are used as catalysts for the oxidation of organic compounds such as toluene and isobutene (Smet *et al.*, 2001; Wang *et al.*, 2008; Nassau *et al.*, 1971; Wenxing *et al.*, 1999). The crystal chemistry of molybdenum compounds is very rich because Mo adopts different oxidation states and therefore forms various coordination polyhedra, such as tetrahedra (Nassau *et al.*, 1971), pyramids (Alonso *et al.*, 2004) and octahedra (Gall *et al.*, 2002). For example, Gall *et al.* (2002) synthesized molybdates $R_4\text{Mo}_4\text{O}_{11}$ ($R = \text{Gd–Tm}$) with an average oxidation state for Mo of +2.5 and explained the stabilization of the crystal structures through the distortion of *trans*-edge-sharing Mo octahedra, based on theoretical calculations. With higher oxidation states Mo forms fivefold oxygen coordination, as in the Dy_2MoO_6 structure (Alonso *et al.*, 2004).

Rare earth molybdates with $M_2(\text{MoO}_4)_3$ stoichiometry exist in several polymorphs, depending on the temperature and the specific rare earth element (Nassau *et al.*, 1971). A high-temperature β -form is stable at temperatures above 1023–1153 K. The transition from the β -modification to the room-temperature α -form is kinetically prevented during cooling and takes place *via* a β' phase, which is metastable at room temperature for a long time. For example, crystals of $\text{Gd}_2(\text{MoO}_4)_3$ exist in the metastable *Pba*2 (Keve *et al.*, 1970) form under ambient conditions for years, although the stable low-temperature form is monoclinic (Nassau *et al.*, 1971). Both the tetragonal and orthorhombic polymorphic modifications contain a network of corner-sharing polyhedra, in which Gd and Mo cations are coordinated by seven and four O atoms, respectively.

Borchardt & Bierstedt (1967) showed that $\text{Gd}_2(\text{MoO}_4)_3$ and the isostructural molybdates of Sm, Eu, Tb and Dy undergo ferroelectric phase transformations in the temperature range $423 \text{ K} < T_0 < 463 \text{ K}$. Gadolinium molybdate, $\text{Gd}_2(\text{MoO}_4)_3$, with a ferroelectric–ferroelastic transition temperature of about 433 K, crystallizes in the space group *Pba*2 (metastable form) below the phase transition and in the space group $P\bar{4}_21m$ above it (Jeitschko, 1972). The paraelectric structure at elevated temperature approaches the average structure of the two ferroelectric–ferroelastic orientations (Jeitschko, 1972). Zou *et al.* (1999) mentioned that the β -modification of $(\text{Nd}_{0.023}\text{Gd}_{0.977})_2(\text{MoO}_4)_3$ with tetragonal symmetry can exist at room temperature.

Dysprosium molybdate, $\text{Dy}_2(\text{MoO}_4)_3$, shows a ferroelectric–ferroelastic transition below 418 K (Roy *et al.*, 1989). According to X-ray powder diffraction, the ferroelectric phase crystallizes in orthorhombic symmetry (space group *Pba*2;

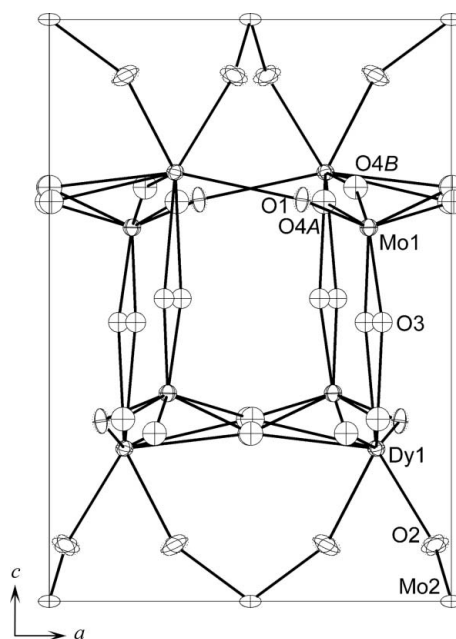


Figure 1
The $\text{Dy}_2(\text{MoO}_4)_3$ tetragonal unit cell, showing the atom-numbering scheme. Displacement ellipsoids are drawn at the 70% probability level.

Roy *et al.*, 1989). Above 1303 K, a reconstructive phase transition into a cubic form of $\text{Dy}_2(\text{MoO}_4)_3$ was reported (Roy *et al.*, 1989; Brixner, 1973).

In this work, single crystals of $\text{Dy}_2(\text{MoO}_4)_3$ have been obtained with the high-temperature β -form tetragonal crystal structure, and the structure refinement based on room-temperature single-crystal X-ray diffraction data has been performed.

According to the single-crystal experiment, dysprosium molybdate shows tetragonal symmetry at room temperature, space group $P\bar{4}2_1m$, with unit-cell parameters $a = 7.295$ (2) Å and $c = 10.578$ (4) Å. On the one hand, the reason for the existence of the tetragonal high-temperature structure at room temperature is not clear, because a monoclinic form of $\text{Dy}_2(\text{MoO}_4)_3$ has been observed below 1043 K (Nassau *et al.*, 1971). On the other hand, the symmetry of the low-temperature forms of related compounds is strongly dependent on the synthesis conditions and cation stoichiometry. For example, for the Nd-substituted phase $(\text{Nd}_{0.023}\text{Gd}_{0.977})_2(\text{MoO}_4)_3$, obtained by the Czochralsky method, a tetragonal crystal structure was found at room temperature by Zou *et al.* (1999). Even a 2% cation substitution of Gd through Nd stabilizes a high-temperature form in the space group $P\bar{4}2_1m$ with $a = 7.356$ (1) Å and $c = 10.685$ (2) Å. The tetragonal $\text{Dy}_2(\text{MoO}_4)_3$ form, obtained in the present work, is stable at room temperature for at least three months (the structure investigation was repeated after three months in storage). The stabilization of the tetragonal structure could be due to a small replacement of Dy by Zr atoms, analogous to $(\text{Nd}_{0.023}\text{Gd}_{0.977})_2(\text{MoO}_4)_3$. However, the refinement of the $\text{Dy}_2(\text{MoO}_4)_3$ structure does not indicate the presence of Zr on Dy sites to within 1% accuracy.

The field stability regions for the various types of $\text{R}_2(\text{MoO}_4)_3$ structures, shown by Nassau *et al.* (1971), depend on temperature and the radius of the rare earth cation. The present $\text{Dy}_2(\text{MoO}_4)_3$ compound is situated between $\text{Gd}_2(\text{MoO}_4)_3$, which has the metastable β' -phase at room temperature, and $\text{Y}_2(\text{MoO}_4)_3$, which has a tetragonal modification in the extended temperature region down to room temperature. The crystal structure of $\text{Dy}_2(\text{MoO}_4)_3$ is formed by corner-sharing MoO_4 tetrahedra and Dy polyhedra coordinated by seven O atoms (Figs. 1 and 2). In this structure, there are two types of Mo tetrahedra, a regular one and a distorted one, with average Mo–O distances of 1.743 (7) and 1.76 (5) Å, respectively. The DyO_7 polyhedron is characterized by Dy–O distances in the range 2.243 (6)–2.393 (5) Å (Table 1), slightly shorter than those for the coordination polyhedron of Gd in the previously published $(\text{Nd}_{0.023}\text{Gd}_{0.977})_2(\text{MoO}_4)_3$ structure mentioned above [2.258 (12)–2.418 (8) Å]. Such compression of the structure can be explained by the slightly smaller size of the Dy^{3+} cation (0.97 Å) compared with the Gd^{3+} cation (1.0 Å), according to the Shannon ionic radii (Shannon, 1976). For another molybdate, Dy_2MoO_6 , with the Mo^{VI} oxidation state, longer Dy–O interatomic distances [2.381 (6), 2.401 (7) and 2.421 (7) Å] lead to an eightfold oxygen coordination of Dy (Alonso *et al.*, 2004).

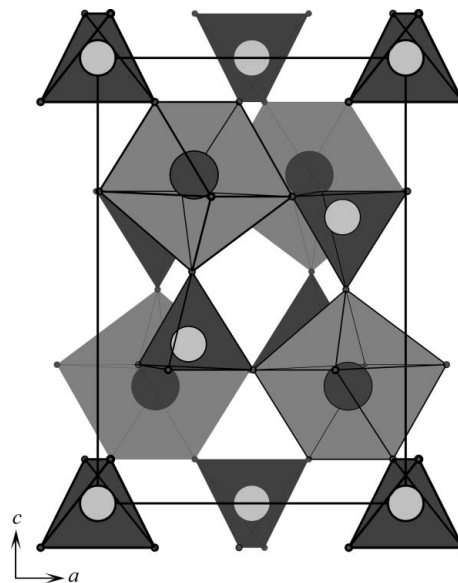


Figure 2

The structural model of $\text{Dy}_2(\text{MoO}_4)_3$, viewed along the b axis. Dark-grey tetrahedra are formed by Mo atoms and light-grey polyhedra by Dy atoms. The positions for atoms O3, O4A and O4B were taken as the average between two close values.

Nassau *et al.* (1971) systematized the crystal structures of $\text{R}_2(\text{MoO}_4)_3$ according to their rare earth ionic radii and oxygen coordination polyhedra RO_x . For example, eightfold oxygen coordination is characteristic for the A family of $\text{R}_2(\text{MoO}_4)_3$ with large rare earth cations such as La, Pr or Pm, and scheelite- or pseudoscheelite-type structures. Due to the shorter Dy–O distances in the tetragonal form of $\text{Dy}_2(\text{MoO}_4)_3$, one would expect a sixfold oxygen coordination of Dy and an orthorhombic crystal structure like $\text{Er}_2(\text{MoO}_4)_3$, but the slightly disordered oxygen positions do not distort the structure symmetry and maintain the DyO_7 coordination. Disordered atoms O3 and O4 make the structure more flexible, atom O3 lying in the vicinity of a mirror plane and atom O4 on a general position. The distance from atom O3 to its mirror image is 0.44 (3) Å, and this seems advantageous for sevenfold oxygen coordination.

The shortest metal–metal distances in the title structure are $\text{Dy1} \cdots \text{Mo1}^{\text{ii}} = 3.7343$ (15) Å, $\text{Dy1} \cdots \text{Dy1}^{\text{ii}} = 3.8572$ (17) Å and $\text{Mo1} \cdots \text{Mo1}^{\text{ii}} = 4.243$ (3) Å [symmetry code: (ii) $-y + 1, x, -z + 1$].

Experimental

Single crystals of $\text{Dy}_2(\text{MoO}_4)_3$ were obtained during an investigation of the Dy_2O_3 – ZrO_2 – MoO_3 phase diagram in an evacuated sealed silica tube from a $\text{Dy}_2\text{Zr}(\text{MoO}_4)_5$ composition by heating to 1273 K, followed by cooling at a rate of 5 K h^{-1} to 1073 K, after which the tube was cooled to room temperature by switching off the heating. From the resulting multiphase polycrystalline mixture, colourless single crystals of $\text{Dy}_2(\text{MoO}_4)_3$ were selected using an optical microscope.

Crystal data

Dy ₂ Mo ₃ O ₁₂	Z = 2
M _r = 804.82	Mo K α radiation
Tetragonal, $P4_21m$	μ = 16.41 mm ⁻¹
a = 7.295 (2) Å	T = 296 K
c = 10.578 (4) Å	0.08 × 0.06 × 0.06 mm
V = 562.9 (3) Å ³	

Data collection

Bruker Kappa APEXII CCD area-detector diffractometer	2641 measured reflections
Absorption correction: multi-scan (SADABS; Bruker, 2004)	723 independent reflections
T _{min} = 0.319, T _{max} = 0.374	645 reflections with I > 2 σ (I)
	R _{int} = 0.054

Refinement

R[F ² > 2 σ (F ²)] = 0.029	$\Delta\rho_{\max}$ = 1.04 e Å ⁻³
wR(F ²) = 0.045	$\Delta\rho_{\min}$ = -0.88 e Å ⁻³
S = 0.97	Absolute structure: Flack (1983),
723 reflections	with 287 Friedel pairs
44 parameters	Flack parameter: 0.02 (2)

Due to the large atomic displacement parameters, a split position from the original position on a mirror plane was introduced for atom O3, with an occupancy of 0.5. Atom O4 was disordered over two sites (O4A and O4B) separated by 0.63 (2) Å. Atoms O4A and O4B were refined with a common displacement parameter and their occupancy factor was constrained to sum to 1. These positions (O3, O4A and O4B) were then refined with isotropic displacement parameters.

Data collection: APEX2 (Bruker, 2004); cell refinement: SAINT (Bruker, 2004); data reduction: SAINT; program(s) used to solve structure: SHELXS97 (Sheldrick, 2008); program(s) used to refine structure: SHELXL97 (Sheldrick, 2008); molecular graphics: DIAMOND (Brandenburg, 2008); software used to prepare material for publication: SHELXL97.

This work was supported by the Deutscher Akademischer Austauschdienst (DAAD) (postdoctoral fellowship grant to SD).

Table 1

Selected bond lengths and contact distances (Å).

Dy1—O2	2.243 (6)	Mo1—O4B	1.697 (13)
Dy1—O3	2.304 (9)	Mo1—O3	1.745 (9)
Dy1—O4A ⁱ	2.307 (15)	Mo1—O1	1.784 (8)
Dy1—O4B ⁱ	2.351 (14)	Mo1—O4A	1.803 (16)
Dy1—O1 ⁱⁱ	2.393 (5)	Mo2—O2	1.743 (7)

Symmetry codes: (i) y, -x + 1, -z + 1; (ii) -y + 1, x, -z + 1.

Supplementary data for this paper are available from the IUCr electronic archives (Reference: LG3065). Services for accessing these data are described at the back of the journal.

References

- Alonso, J. A., Rivillas, F., Martínez-Lope, M. J. & Pomjakushin, V. (2004). *J. Solid State Chem.* **177**, 2470–2476.
- Borchardt, H. J. & Bierstedt, P. E. (1967). *J. Appl. Phys.* **38**, 2057–2061.
- Brandenburg, K. (2008). *DIAMOND*. Crystal Impact GbR, Bonn, Germany.
- Brixner, L. H. (1973). *J. Cryst. Growth*, **18**, 297–302.
- Bruker (2004). APEX2 (Version 1.08), SAINT (Version 7.03) and SADABS (Version 2.11). Bruker AXS Inc., Madison, Wisconsin, USA.
- Flack, H. D. (1983). *Acta Cryst.* **A39**, 876–881.
- Gall, P., Barrier, N., Gautier, R. & Gougeon, R. (2002). *Inorg. Chem.* **41**, 2879–2885.
- Jeitschko, W. (1972). *Acta Cryst.* **B28**, 60–76.
- Keve, E. T., Abrahams, S. C., Nassau, K. & Glass, A. M. (1970). *Solid State Commun.* **8**, 1517–1520.
- Nassau, K., Shiever, J. W. & Keve, E. T. (1971). *J. Solid State Chem.* **3**, 411–419.
- Roy, M., Choudhary, R. N. P. & Acharya, H. N. (1989). *J. Therm. Anal.* **35**, 1471–1476.
- Shannon, R. D. (1976). *Acta Cryst.* **A32**, 751–767.
- Sheldrick, G. M. (2008). *Acta Cryst.* **A64**, 112–122.
- Smet, F. D., Ruiz, P., Delmon, B. & Devillers, M. (2001). *J. Phys. Chem.* **105**, 12355–12363.
- Wang, X., Xian, Y., Wang, G., Shi, J., Su, Q. & Gong, M. (2008). *Opt. Mater.* **133**, 33–39.
- Wenxing, K., Yining, F., Kaidong, C. & Yi, C. (1999). *J. Catal.* **186**, 310–317.
- Zou, Y.-Q., Chen, L., Gao, X.-Y., Tang, D.-Y. & Luo, Z.-D. (1999). *Chin. J. Struct. Chem.* **18**, 447–450.